

SOME FUNDAMENTAL ASPECTS OF PULP SCREEN CAPACITY

*H.J. Salem^{1,2}, R.W. Gooding^{1,2,4}, D.M. Martinez^{2,3}
and J.A. Olson^{1,3}*

¹ Department of Mechanical Engineering
The University of British Columbia
6250 Applied Science Lane
Vancouver, British Columbia, Canada V6T 1Z4

² The Pulp and Paper Centre
The University of British Columbia
2385 East Mall
Vancouver, British Columbia, Canada V6T 1Z4

³ Department of Chemical and Biological Engineering
The University of British Columbia
2360 East Mall
Vancouver, British Columbia, Canada V6T 1Z3

⁴ Aikawa Fiber Technologies
5890 Monkland Avenue, Suite 400
Montreal, Quebec, Canada H4A 1G2

ABSTRACT

Pulp screens remove contaminants from pulp suspensions and are critical to the production of high-quality paper products. Screen performance is determined by two internal components: a cylinder with apertures that pass acceptable fibres and block oversize contaminants, and a rotor that clears the apertures of any blockages. Capacity is an essential parameter of screen operation and a necessary consideration in evaluating changes made to enhance debris removal or reduce power consumption. The present study uses a pilot pulp screen to assess capacity limits, and a specialized laboratory screen with a high-speed video camera to study what happens at a screen aperture.

What results is an understanding of some mechanisms related to the deposition and removal of fibres at an aperture where there is a time-varying flow bifurcation, and which is proposed herein as the essence of screen capacity.

INTRODUCTION

Pulp Screens

Pulp screens remove fibre bundles, plastic specks and other oversize contaminants from pulp suspensions before pulp is made into paper. Virtually every pulp and paper mill has screens and they not only enhance the cleanliness of paper products, but increase the flexibility and economy of the pulping processes. Pulp screens promote a higher level of paper recycling through their ability to remove a wide range of contaminants at relatively low cost. They remove shives and fibre bundles from kraft pulp and minimize requirements for more expensive chemical bleaching treatments. Screens also fractionate mechanical pulp so that acceptable fibre can be fed forward without further refining, thus saving energy and preserving fibre strength.

A typical pulp screen is shown schematically in Figure 1. This pulp screen is also known as a “pressure screen” to distinguish it from older-style screens that now exist in only a small number of pulp mills. The present study is made in the context of these modern pressure screens. The screen receives a feed stream of pulp and separates this stream into an accept stream of cleaned pulp and a reject stream where contaminants are concentrated. The operating consistency of pulp screens is typically in the range of 1% to 5% and approximately 10 to 30% of the volumetric feed flow will leave through the reject outlet.

Within the pulp screen is a screen cylinder that acceptable fibres pass through but oversize contaminants do not. Apertures in the cylinder are in the form of slots or holes and the size of these apertures is, as one would expect, the most critical variable in pulp screen design. Smaller apertures will increase the removal efficiency of contaminants, but may also lead to a reduction in screen capacity. Screening technology is challenged by a range of industry forces: Increasingly high contaminant levels in recycled furnishes coupled with publisher demands for greater cleanliness creates the need for smaller screen slots. Slots as narrow as 80 to 100 microns, i.e. just three or four fibre diameters wide, can be found in use, though slot widths are more typically in the range of 150 to 250 microns.

A breakthrough in pulp screening occurred in the 1980s with the development of “contoured” screen cylinders. The contours describe a feature whereby the

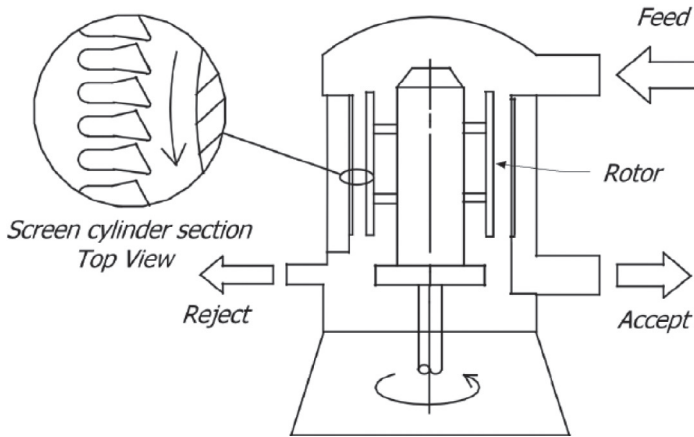


Figure 1. Schematic drawing of a pulp screen.

entry to a screen aperture is located within a recess on the cylinder surface. The width, depth and shape of these recesses have been the subject of significant study and industrial development. An example of a typical contoured cylinder surface is shown in Figure 2. The presence of contours increases screen capacity several-fold, as is discussed below along with a consideration of the fundamental mechanisms underlying the action of the contours.

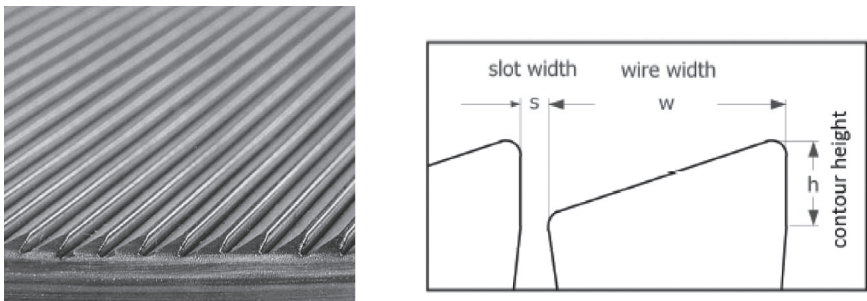


Figure 2. A close-up view of the feed-side of an industrial screen cylinder showing: (a) multiple slots and a contoured surface (left); and (b) a schematic view of a single slot as defined by two adjacent wires (shown only in part) that create the contour (right) where s is the slot width (mm), w is the wire width (mm) and h is the contour height (mm).

The screen rotor is the other performance component of a pulp screen, and the rotor works in concert with the cylinder. Two typical examples are shown in Figure 3. The primary role of the rotor is to keep the screen cylinder apertures clear of any fibres or contaminants that could plug the apertures and cause the screen to fail. A rotor is thought to work in three ways: 1) generating pressure pulsations that backflush the apertures of any incipient blockages, 2) accelerating the pulp suspension on the feed side of the cylinder to a high tangential velocity and 3) inducing turbulence at the cylinder surface.

Various rotor designs have been developed over time, but they share the common characteristic of having a foil or element or some feature that protrudes from the rotor and passes with a clearance of 3 to 7 millimeters from the screen cylinder surface. Given that there is no contact with the cylinder surface, the rotor is assumed to rely on a hydrodynamic effect to clear the screen apertures rather than any scraping or wiping action.

Screen performance is characterized by a number of parameters: Screen capacity is the accept tonnage of the screen. Debris removal efficiency is the percentage of contaminants removed from the feed stream and directed to the reject stream, which one naturally seeks to maximize. The mass reject ratio is percentage of the fibre mass flow in the feed stream that passes to the reject stream and which is to be minimized to avoid the loss of good fibre. Fibre fractionation refers to a shift in the fibre length distribution between the feed, accept and reject

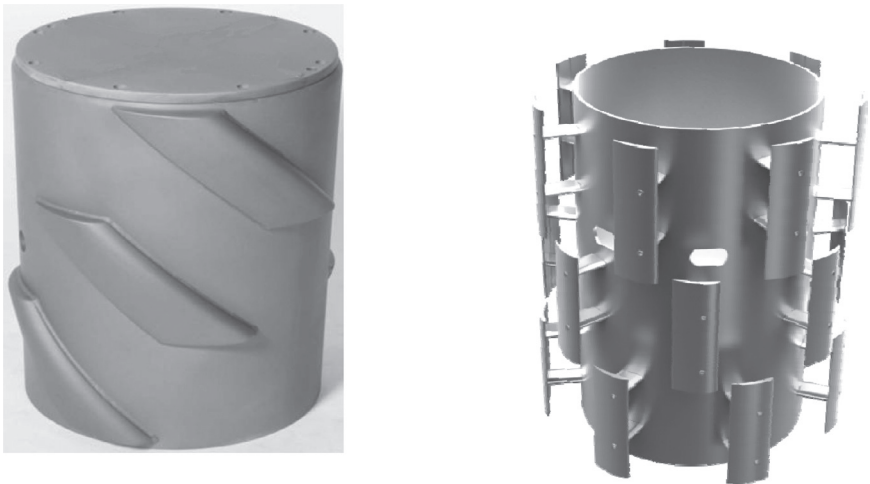


Figure 3. Two typical pulp screen rotors: (a) a “closed” rotor with a solid core (left) and (b) an “open” rotor (right) with foils.

streams and which one seeks to minimize in some industrial applications and maximize in others. Power consumption is roughly proportional to the cube of rotor tip speed, and there is a drive to reduce power as part of larger power conservation programs at pulp mills. “Runnability” is an important, but somewhat qualitative parameter, which relates to the ability of the screen to operate reliably even with the unavoidable variations in pulp consistency and character in mill operations.

Screen Capacity

Screen capacity is perhaps the most important screening parameter given mill requirements to produce large amounts of commodity products on an ongoing basis. One thus seeks to avoid having the screen system as a bottleneck to production. Capacity is also a reflection of robust screen operation and may indicate that smaller, more efficient, apertures or a lower rotor speed may be used without limiting mill operation.

The definition of screen capacity is, as noted above, most commonly taken as the maximum accept mass flow rate. Feed consistency is typically set by other processes in the mill system, and the consistency drop from the feed-to-accept stream is relatively small. It is therefore useful to discuss capacity in terms of the maximum volumetric accept flow rate at different feed consistencies. This also serves to separate the flow (hydraulic) effects from consistency (fibre network) effects and supports an independent and fundamental understanding of each factor. Capacity will naturally increase as the “open area” of the screen cylinder through which flow can pass increases, which reflects both a simple increase in the size of the cylinder and changes in the width and spacing of slots, for example. Slot width is often specified for a particular screen application to ensure a particular level of contaminant removal. Thus, in a further attempt to distill the industrial process to more primitive terms and support more fundamental study, the issues of total screening area and open area will be set aside to consider increased capacity in terms of maximum slot velocity.

Slot velocity, as commonly used in the present study, will be the time-averaged, slot-averaged and cylinder-averaged value. Dynamic variations in slot velocity will be studied herein, but this is done in support of increasing the overall time-averaged velocity. Likewise the consideration of spatial variations of slot velocity across the width of the slot will be made to elucidate the factors underlying screen capacity. A two-dimensional approach is taken in this study, based on the simplifying assumption that velocity variations and mechanisms occurring along the length of the slot are of secondary importance. Industrial screen cylinders are in the order of 600 mm in both length and diameter and there are local variations in slot velocity and consistency, but these second-order effects are set aside to

simplify the current study. Thus, the terms “screen capacity” and “slot velocity” will be used somewhat interchangeably herein.

Capacity-Defining Mechanisms

The limit of screen capacity in an industrial sense is commonly signaled when the feed-accept pressure differential exceeds a prescribed limit. There are two typical scenarios: In the first, a “healthy” screen demonstrates an increase in pressure differential proportional to the square of the accept flow rate which typifies the flow resistance relationship for turbulent flow and a flow restriction with a constant pressure drop coefficient. More commonly, however, one will encounter the second scenario, where the pressure differential increases roughly with the square of the accept flow rate until the point where incipient aperture plugging is thought to occur. At this point the accept flow decreases – even as the pressure differential is increasing. Some studies of hydraulic capacity have determined that fibres immobilized within a slot have a predominant effect in determining the pressure drop coefficient during normal operation as well as during failure.

The presence of slot plugging is shown in Figure 4. In practice, the fibrous plugs that fill the slot may be either loosely or tightly compressed. Modes of slot plugging include fibre trapping, fibre stapling, floc compression and reverse-side plugging. Trapping is shown in Figure 4b as fibres accumulate on the downstream edge of the slot. If not removed, fibres will stack upon each other

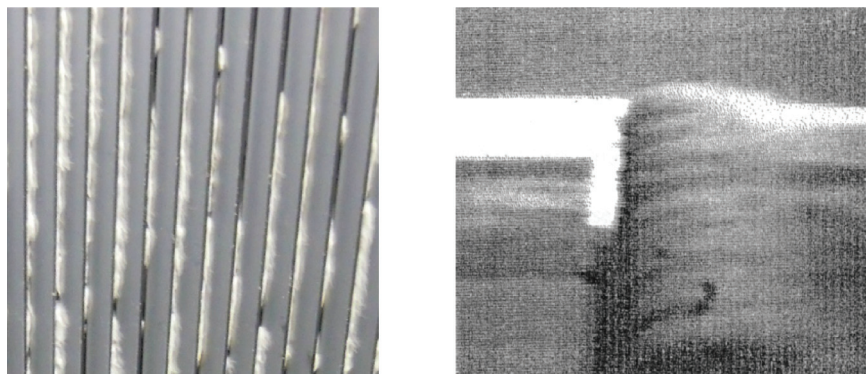


Figure 4. Slot plugging phenomenon as seen: (a) in a feed-side view of several slots in a plugged cylinder (left), and (b) in a laboratory flow channel (right) with a side view of a single, partially-plugged slot with fibres trapped on the downstream edge of the slot.

until the slot is filled. Fibre stapling is a related effect wherein the fibre straddles two adjacent slots. Floc compression is considered to occur in high-consistency screening situations where fibre flocs are not dispersed before entering the slots, which are typically several times narrower than the floc diameter. Reverse-side plugging is thought to arise where a very strong suction pulse from the screen rotor draws fibres into the slot from the accept side of the screen cylinder and wedges the fibres and flocs there. The present study is focused on the most common and most industrially-significant mode of failure, which is thought to be a result of fibre trapping.

Industrial Relevance

Capacity is a function of fibre length, consistency, aperture size and geometry, rotor speed and rotor type. Increased demands on screening technology have come from many of the current trends in industry: The need to increase production in older mills without adding equipment has led to increases in both slot velocity and feed consistency so that some screens now operate with consistencies over 4% and slot velocities in the range of 3 to 5 m/s. At the same time, the need to reduce energy consumption has led to reduced rotor speeds. Small slots, higher consistencies, higher slot velocities and lower rotor speeds all come back to the challenge of understanding the limitations of screen capacity and using that understanding to enhance equipment design and operation.

Objective and Approach

The goal of this study is to develop a fundamental understanding of what determines the capacity of modern pulp screens. The approach that will be taken is to:

- Review the relevant literature related to pulp screening topics, as well as fibre motion and fibre flocculation.
- Assess capacity in a small, industrial pulp screen under controlled conditions, and thus to understand how rotor speed, pulp consistency, slot geometry and other factors affect the maximum slot velocity.
- Consider the essential mechanisms of fibre accumulation and removal experimentally, using a laboratory device which recreates key aspects of the pulp screen flows and permits observation of the phenomena using high-speed photographic techniques.
- Propose a model of fibre accumulation that follows from the flow environment in a pulp screen and the fibre trapping phenomenon. A more fundamental understanding of the essential fibre trapping mechanism is developed theoretically.

LITERATURE REVIEW

Flow of Fibres Near a Screen Wall

Gooding and Kerekes [1] used high-speed photography to record the trajectories of fibres near a single slot in a cross-flow. They identified the existence of a layer with low fibre concentration adjacent the wall upstream of the slot. The associated “wall effect” was one of the factors limiting fibre passage. They also observed that under certain flow conditions, fibres became trapped on the downstream edge of the slot. Kumar [2] assessed the effect of fibre length, slot width and flow velocities on the probability of fibre passage experimentally. He found that fibre passage varied with the ratio of fibre length to slot width. This work was later investigated by Olson and Wherrett [3] who confirmed that fibre passage can be characterized by the single function proposed by Kumar.

Yu and DeFoe [4] studied the flow patterns at the feed-side surface of smooth and contoured screen cylinders under steady flow conditions. They speculated that fibre mats containing fibres and contaminants can form on the surface of the cylinder and that these mats remixed and were diluted during screen operation. In a further study, Yu and DeFoe [5] showed that for contoured cylinders, a vortex flow is an effective means of preventing fibres from residing on slot openings or stapling between two openings. As discussed previously, “stapling” is a mechanism in which the two ends of a fibre are drawn into adjacent apertures with the fibre immobilized on the land area between the slots [6].

Gooding [7] examined the flow patterns and turbulence levels of various smooth and contoured screen slots in a steady cross-flow to obtain a mechanistic understanding of what determines the slot-based flow resistance and the conditions that lead to minimum values of resistance. He also observed how fibres build up within the slot and considered the contribution of the incipient fibre blockages to flow resistance. The concentration and orientation of fibres in a turbulent flow near a smooth wall was assessed by Olson [8] and found to be a function of fibre length. Yong *et al.* [9] used high-speed video photography to determine the trajectory of nylon fibres approaching narrow screen apertures in a laboratory pulp screen.

The more general topic of turbulent flow over a rough wall has been studied extensively because of its importance in a range of industrial applications [10, 11, 12, 13].

Effect of Wall Geometry, Local Flows and Flocculation on Fibre Screening

Screen cylinder contours have an important effect on screening efficiency and capacity. Heise [14] recommended the use of screen cylinders that minimize turbulence between the rotor and the screen surface in order to maximize screening

efficiency. Niinimäki *et al.* [15] found that the efficiency of “probability screening” is more dependent on contour roughness than on slot width. Increasing the contour height led to an improvement in screen capacity and a reduction in debris removal efficiency.

Halonen *et al.* [16] defined fluidization as a process of loosening fibre contacts inside flocs. Depending on the conditions and properties of the pulp adjacent to the contoured screen surface, the fluidized state may extend the cleansing effect induced by the rotor according to Frejborg [17]. Bliss [18] agreed with the idea of extended fluidization and stated that turbulence allows the openings to pass more fibres after the cleaning pulse of the rotor in the case of a contoured screen cylinder surface than for a smooth surface.

Mokamati *et al.* [19] developed a Computational Fluid Dynamic (CFD) simulation of the flow through a screen slot and considered the effect of various screen contours. As contour height increased, turbulence intensity near the wall increased. Turbulence intensity also increased with decreasing wire width suggesting that the ratio of contour height to wire width controls the boundary layer thickness and turbulence intensity near the wall.

Yu *et al.* [20] showed that the aperture size in a screen cylinder was the dominant factor affecting contaminant removal efficiency. As one would expect, the larger the aperture size, the lower the contaminant removal efficiency and the higher the volumetric and mass throughput.

Kerekes [21] investigated the behaviour of pulp flocs at the entry to constrictions using high speed cine photography. The elongational strain imposed by the accelerating flow in the entry stretched the floc but did not rupture it. When flocs did rupture, they did so by tensile stretching rather than by shear. On entering the constriction, fibres did not maintain their relative lateral position perpendicular to the flow direction; rather, they tended to concentrate along the wall of the constriction, making subsequent floc dispersion more difficult. Blaser [22] observed the behaviour of preflocculated ferric hydroxide flocs subjected to either a simple shear flow or a two-dimensional straining flow. He found that the simple shear flow led to rotation of the flocs. In the extensional flow, no continuous rotation occurred and flocs were broken apart along the axis of straining.

Paul *et al.* [23] showed that the use of viscous liquid as the suspending medium increased screen capacity. The maximum mass flow rate, i.e. maximum aperture velocity, increases as the suspending medium viscosity increases. The reduction in floc size in more viscous liquids produces a decrease in the pressure loss across the screen cylinder. The exit layer height increases with increasing viscosity at constant average accept and rotor velocities. The exit layer was noted by Gooding [1] and was mathematically analyzed by Olson and Kerekes [24], and is especially significant given that fibres within this layer are candidates to pass through screen apertures [1,2].

Effect of Rotor on Screen Flows

Rotor design is critical in determining pulp screen performance. The effects of pressure pulse magnitude, pulse width and frequency on capacity are not, however, well understood. Karvien and Halonen [25] assessed pressure pulsations using experimental and computational techniques for a foil-type rotor. They speculated that the backflushing action of the pressure pulse arose from a “Venturi effect” created by the acceleration of the flow through the gap between the moving rotor tip and stationary screen surface. This acceleration causes the local pressure on the feed side of the screen cylinder to decrease to the point that there is a reversal in the flow through the aperture. Pinon *et al.* [26] measured the pressure pulse in a laboratory pulp screen. Their results showed that increased rotor speed increased pulse strength. Although increased rotor speed shortened the duration of the pulse, the shape of the pulse was relatively unchanged.

Levis [27] found that a wider gap between the foil and screen surface leads to increased debris removal efficiency, albeit with lower capacity. Niinimäki *et al.* [28] found that screen capacity is sensitive to changes in the foil “angle of attack” and thus foil angle could be varied to optimize screen performance.

Feng *et al.* [29] simulated the pressure pulse using CFD and compared the results to experimental measurements over a wide range of foil tip speeds, clearances, angles-of-attack, and foil cambers. The pressure pulse peak was found to increase linearly with the square of tip speed for all angles-of-attack studied. The positive pressure peak near the leading edge of the foil was eliminated for foils operating at a positive angle-of-attack. The results also showed that the magnitude of the negative pressure peak increased as clearance decreased.

The effect of varying pulse frequency on rotor performance was studied numerically and experimentally by Delfel *et al.* [30] using a novel foil rotor. The results showed that a two-foil rotor had greater capacity and reduced power consumption in comparison to a three-foil rotor with identical foil geometry. The CFD model they introduced anticipated a back-flush flow caused by the acceleration of the flow under the foil. However, they used a solid wall boundary condition rather than modelling the slots in the cylinder.

In general, most published work has focused on the effect of flow on screen performance without taking into full account such industrial factors such as the effect of the fibre network or contour geometry. More importantly, the published work has not led to a detailed and rigorous understanding of either fibre accumulation or the hydraulic aperture-clearing mechanism which are critical to reliable screen operation.

Screen Capacity

While a number of studies have been conducted to understand the factors affecting pulp screen performance, only a few were focused on factors affecting the capacity of pulp screening [6, 31, 32, 33, 34]. Niinimäki [35] categorized the matting of fibres on the inner surface of the screen, and the pulsation and backflow induced by the foils as macro phenomena, and the hydrodynamic forces exerted on the fibres and fluidization due to turbulence on the screen surface as micro phenomena. Contoured screen cylinders are thought to enhance the turbulence conditions on the screen surface and can extend the cleansing effect induced by the rotor [17]. It is widely believed that the rotor pulses serve, at least in part, to disrupt the fibre mat and lift trapped particles away from the screen apertures [35].

Martinez *et al.* [32] introduced a screen capacity model by assuming that screen blinding limits volumetric capacity and that blinding occurs when a fibre floc becomes immobilized in a screen slot. The essential analysis is a force balance on a single floc in a slot with the forces arising from the flow through the slot, the friction of the floc against the slot walls, and the rotor pulsation. However, this model does not embrace important factors such as rotor pulse frequency, fibre length distribution, rotor wake effects and fibre trapping.

Hamelin *et al.* [34] conducted a series of pilot screening trials for a range of foil configurations. For each rotor configuration, the maximum slot velocity-power curve was determined by setting the rotor speed to a constant value and increasing the slot velocity until the onset of plugging. In a similar way, Konola *et al.* [36] assessed the operating region for two commercial rotors in an industrial setting, and plotted the maximum slot velocity versus rotor tip speed. Some results from Konola *et al.* are shown in Figure 5, which suggests a fairly linear relationship between the maximum slot velocity and rotor tip speed, with the operating region located below the lines.

The body of literature described above extends from industrial screen performance to a more fundamental observation of fibre motion near walls. The next step in the study was to recreate some key aspects of industrial pulp screening in a laboratory environment, where the effects of various key variables could be assessed.

EXPERIMENTAL STUDY OF PILOT SCREEN CAPACITY

While industrial studies can provide context and can identify some of the principal factors that determine capacity, pilot plant studies are useful to make more precise measurements in a controlled environment. A pilot plant screen

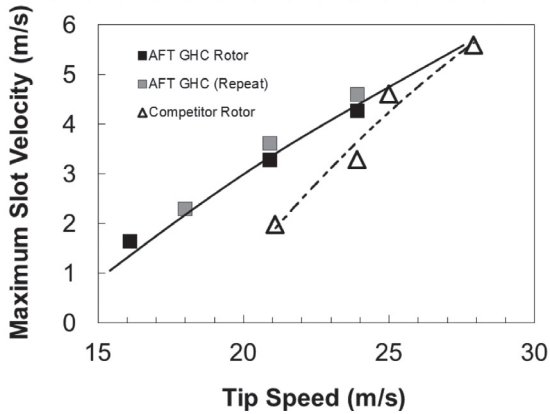


Figure 5. Pilot plant data showing the maximum slot velocities for two commercial rotors (M200 pulp screen, 3.1% consistency softwood pulp, 0.20 mm slot) [36].

can also be used to assess factors which would impractical in an industrial environment. The current study considered the influence of cylinder geometry, pulp type, rotor speed and flow velocities on screen capacity. In particular, five types of screen cylinders with different slot geometries were tested using different softwood/hardwood kraft pulp blends and different volumetric reject ratios.

Experimental Methodology

Experiments were conducted using a Beloit MR8 pulp screen (Figure 6) located in the pilot plant of The University of British Columbia Pulp and Paper Centre. The MR8 is a small, industrial pulp screen with screen cylinders measuring 203 mm in diameter and 254 mm in length. This compares in size to a typical industrial cylinder which might be 600 mm in diameter and 600 mm long. The MR8 screen was equipped with a variable frequency drive (VFD) to vary rotor speed up to a maximum tip speed of 20 m/s. Industrial screens typically operate at speeds as high as 30 m/s, but the range of 12 to 20 m/s reflects the current industrial interest where lower speed offers the benefits of reduced energy, extended equipment lifetime and increased contaminant removal efficiency. An AFT EP™ foil rotor of the type shown in Figure 3b was used for all trials and the rotor-cylinder gap was set at 4 mm. Pulp was supplied from a 1500 litre tank using a centrifugal pump. The reject and accept streams from the screen were returned to the feed tank to permit extended operation of the flow loop. Flow meters and flow control valves were on the feed, accept and reject lines. Pulp temperature was

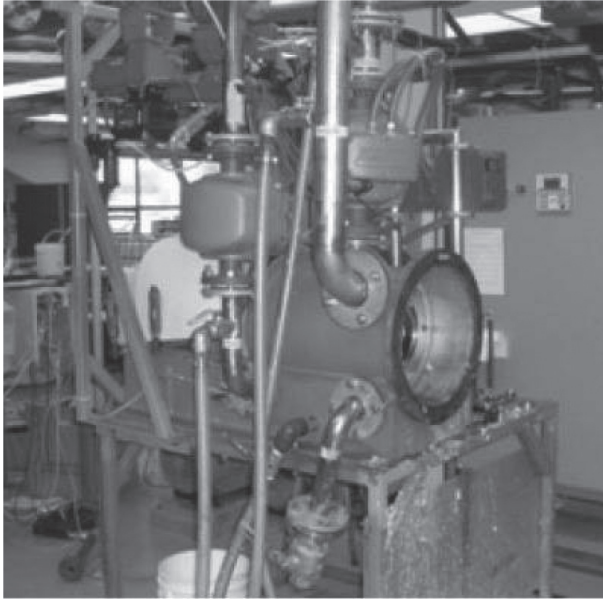


Figure 6. The UBC MR8 pilot pulp screen and associated flow loop. The cover has been removed from the screen in this photo. Note that the MR8 screen is oriented horizontally versus the more typical vertical orientation shown in Figure 1.

maintained at a nominal value of 40 degrees C using a 5 kW electric heater installed in the feed tank. The volumetric reject ratio was maintained at 20% in most tests, which is a typical industrial value and provides minimal reject thickening and risk of reject line plugging.

Five screen cylinders were tested in this study, as listed in Table 1. In certain cases, circumferential sections of the of the cylinders were blinded off to provide equivalent open areas, and thus to ensure an equivalent accept flow rate through the piping system for equivalent slot velocities.

The pulp used for most of the tests was a blend of reslushed hardwood (HW) and softwood (SW) kraft market pulps. A 50/50 blend was typically used following on previous studies that used this ratio to simulate simulate a deink pulp [37]. The ratio of hardwood and softwood pulp components was varied as part of the experimental program to assess the effect of fibre length distribution on screen capacity.

The trial protocol was to operate the screen at a particular slot velocity and maximum rotor speed of 20 m/s and then to reduce rotor speed until there was a

Table 1. Cylinder Characteristics

<i>Cylinder Designation</i>	<i>Contour height (mm)</i>	<i>Wire width (mm)</i>	<i>Slot width (mm)</i>	<i>Open area (m²)</i>
A	1.2	3.2	0.15	0.00453
B	0.9	3.2	0.15	0.00453
C	0.6	3.2	0.15	0.00453
D	0.6	2.3	0.15	0.00619
E	0.6	3.2	0.10	0.00482

rapid increase in the feed-accept pressure differential which signified that the screen had plugged. Rotor speed was then returned to 20 m/s, the slot velocity was increased by 0.5 m/s and the procedure was repeated. A plugging/capacity boundary for the minimum rotor speed was thus generated for different cylinders, pulp types and consistencies. It was found that minimum rotor tip speed needed to prevent plugging was repeatable within ± 0.2 m/s, which is small relative to the effect of changes in rotor speed.

Experimental Results

Consistency Effects

The plugging boundary for a typical pulp screen cylinder (Cylinder B) is shown in Figure 7 as a function of the feed pulp consistency. The data show that the relationship between V_r , rotor tip speed (m/s), and maximum V_s , slot velocity (m/s), is strongly linear, consistent with the relationships reported previously [36] and shown in Figure 5. One may thus propose a simple equation for the capacity:

$$V_s^* = C_1 + C_2 V_r \tag{1}$$

where V_s^* is the maximum value of V_s at a particular value of V_r and which thus defines the plugging boundary/limiting curve.

Higher consistencies cause the limiting curve to shift downward and to the right, i.e. a higher rotor speed is required to maintain a certain maximum slot velocity. For example, increasing consistency from 1.0% to 2.0% requires rotor speed to increase from 10.8 to 13.6 m/s to provide a maximum slot velocity of 3 m/s. Such a trend is reasonable, and in comparing these results to Figure 5, one sees that the higher consistency of 3.1% leads to rotor speeds in the range of 19 to 23 m/s (depending on the rotor design) to provide a 3 m/s maximum V_s . Thus the results of the two experiments are generally consistent despite differences in rotor type and pulp furnish. One sees in Figure 7 that a 2.0% consistency also prescribes

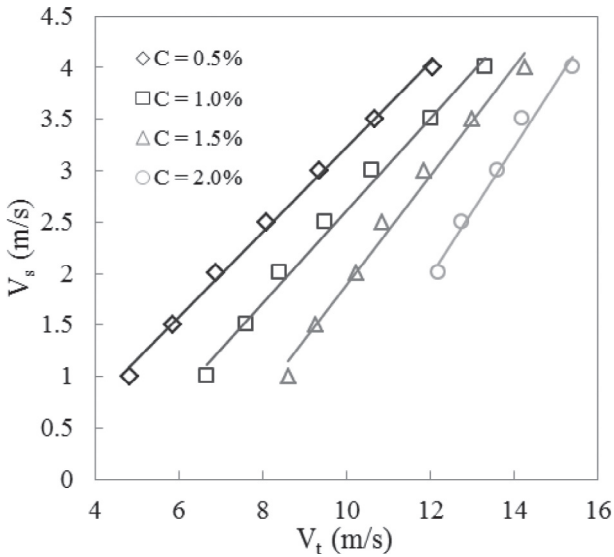


Figure 7. The effect of feed consistency on maximum slot velocity (Cylinder B) where the region below the line represents the operating region of the pulp screen and the line is the plugging boundary.

a minimum V_s of 2 m/s. This is due to issues related to the passage ratio of pulp at low V_s [38], elevated reject line consistency and some problems with reject line plugging, which is considered here as an experimental artifact and somewhat distinct from the issue of screen cylinder plugging.

Pulp Furnish Effect

The effect of pulp furnish on capacity was assessed by mixing softwood and hardwood kraft pulp in different proportions. The results are shown in Figure 8 for Cylinder B and for a feed consistency of 1.0%. The linearity seen in Figure 7 is preserved. Increased proportions of softwood pulp leads to a shift of the curve downward and to the right. In particular, replacing the hardwood pulp with a softwood pulp requires an increase in rotor speed from 9.4 m/s to 11.5 m/s to maintain a maximum V_s of 3 m/s. This is comparable to the increase seen in Figure 7 when consistency is doubled. By back-calculating from the constituent fibre length distributions, one sees that a switch from the hardwood to softwood furnish also doubles the amount of mass of longer fibres (i.e. greater than 0.7 mm long).

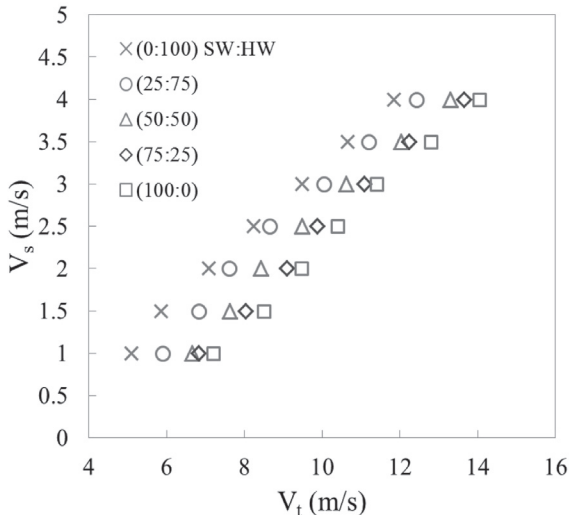


Figure 8. The effect of furnish blend (fibre length distribution) on maximum slot velocity (Cylinder B; 1% feed consistency).

Contaminant Concentration Effect

Increased contamination levels have been speculated to reduce capacity. This follows on a model that considers a contaminant becoming lodged in a screen slot, becoming a site for the accumulation of fibres, and the blockage growing along the slot until the cylinder becomes completely blocked. Slot-wise growth of fibre blockages has been observed in laboratory screens. There is also anecdotal evidence of pilot plant screens (which typically use clean, reslushed pulps) having significantly higher capacities than industrial screens.

A trial was thus conducted using the MR8 screen with 1.5% feed consistency, Cylinder B and a slot velocity of 2.0 m/s. Mill debris, i.e. heavily contaminated material gathered from the reject stream of the third stage of a mill screen system treating old corrugated containers (OCC), was added to a 50/50 hardwood/softwood pulp blend and the minimum rotor tip speed to maintain reliable screen operation was assessed. No significant effect on capacity (i.e. minimum rotor tip speed) was seen even when as much as 12% of the feed suspension was comprised of the mill debris. The minimum rotor tip speed was sensitive to the addition of cubical polyethylene specks, but even a very high (2%) loading level led to only a modest increase in minimum rotor speed. The specks generally ranged from 0.5 to 2.0 mm in nominal diameter.

Cylinder Geometry Effects

Increased contour height is commonly assumed to increase capacity. While Figure 9 shows that this is true at very low rotor speeds, the benefit of increased contour height appears to disappear, or at least to be substantially diminished, in the range of industrial interest (i.e. above 12 m/s). This lack of benefit is somewhat surprising, but it may be that the contour height is of significant benefit at consistencies higher than the 1.5% consistency tested here.

Slot width is also expected to lead to significant reductions in capacity, and that is seen in Figure 10. The figure also shows that a narrower slot “pitch” (i.e. the distance between slots) also causes reduced capacity. This is likely to due to the presence of the softwood pulp and potential for slot-to-slot stapling given that over 60% of the fibre mass are candidates for stapling, which is far above the levels at which stapling is expected to occur [6].

Summary of Pilot Screen Capacity Findings

Tests were done on a pilot-scale MR8 pulp screen to determine the influence of screen cylinder, pulp and flow variables on capacity. Significant reductions in

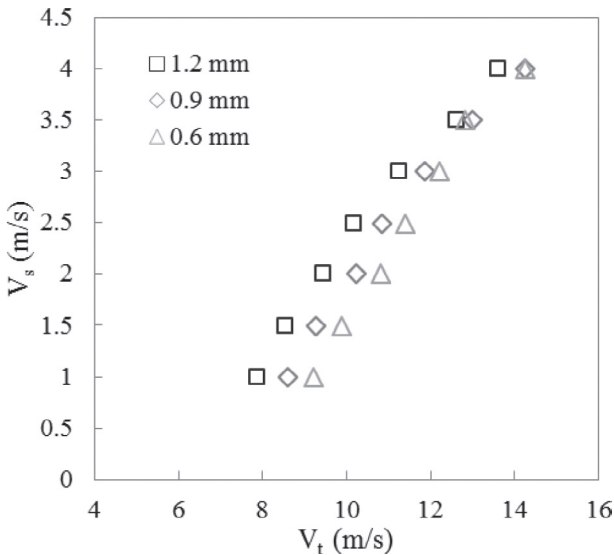


Figure 9. Contour height is seen to be beneficial at very low rotor speeds, but the benefit appears to disappear as the speed enters into the range of commercial interest (i.e. above 12 m/s). Data are for Cylinder B, a 50/50 hardwood/softwood blend and 1.5% feed consistency.

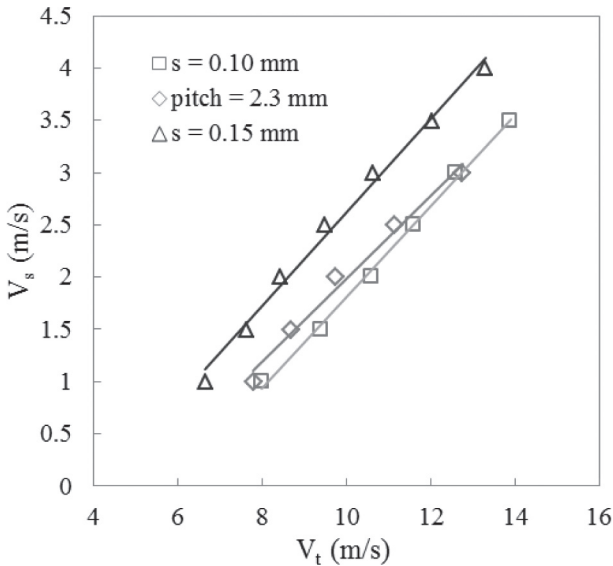


Figure 10. Narrower slots and reduced slot pitch each led to reduced capacity (50/50 hardwood/software blend; 1.0% feed consistency). Cylinder B is the reference cylinder with $s = 0.15$ mm. Cylinder D has $w = 2.3$ mm. Cylinder E has $s = 0.10$ mm.

capacity occurred when long fibre concentration was increased – either from an increase in consistency or from a shift in the fibre length of the furnish. Smaller slots also led to reduced capacity. Despite industrial practices, contour height did not lead to increased capacity.

EXPERIMENTAL STUDY OF SLOT PLUGGING

Following on the pilot plant study described above, one can consider a more focussed examination of phenomena that may be of essential importance to screen capacity. The previous section revealed fibre concentration to be a significant factor in limiting capacity. It follows that capacity may be defined by the balance between fibre deposition and removal rates. Such mechanisms will be examined herein.

In particular, this section considers the turbulent cross-flow of a two-phase fluid within a moving upper boundary, and a contoured, slotted lower boundary – or in other words, the flow of pulp fibres within the upper boundary defined by the screen rotor and the lower boundary by a screen cylinder, with successive flow

bifurcations providing the flow through the screen cylinder slots. High-speed videography provided qualitative and quantitative information on fibre motion at the slot entry, the flow field within the screen contour, and dynamic flows induced by the passage of the rotor.

Three types of tests were conducted with using a laboratory screening device:

- qualitative observations of fibre trapping and other fibre motion phenomenon, made using a dilute suspension of pulp fibres,
- quantitative measurements of steady flow velocities adjacent the screen cylinder surface using particle velocimetry (PIV) techniques and a dilute suspension of pulp fines, and
- quantitative measurements of unsteady flows associated with the passage of the rotor foil near the screen slots.

Experimental Methodology

Experiments were conducted with using a cross-sectional screen (CSS) and Phantom™ high-speed video camera. The CSS is a laboratory-scale screen modelled on the cross-section of a Hooper PSV 2100 pulp screen [9, 26, 29, 39]. The CSS has a depth of 50 mm and the partially-slotted cylinder has an inside diameter of 290 mm, as shown schematically in Figure 11. Feed flow is supplied from a 150 litre reservoir. Accept and reject flows are controlled using magnetic flow meters, flow control valves and a LabView™-based control system. Two rotors were used in this study: The one used for most tests was modelled on an

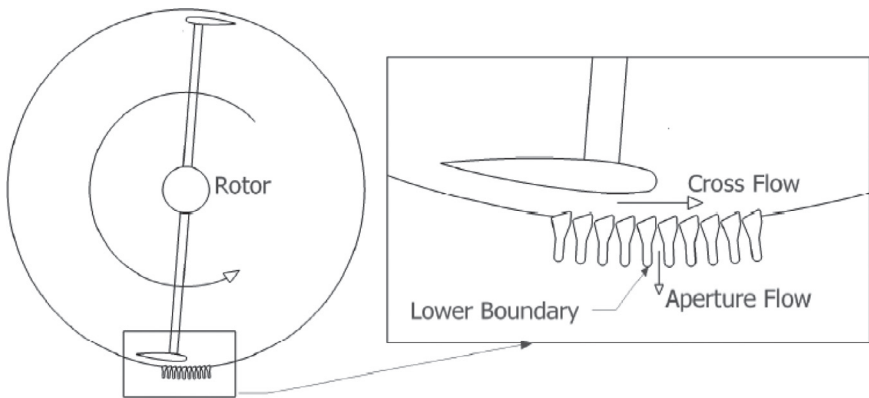


Figure 11. Schematic drawing of the CSS (left) and slotted coupon (right) which simulates the flows through the slots in a pulp screen cylinder.

Table 2. CSS Coupon Geometry

<i>Designation</i>	<i>Contour height, h (mm)</i>	<i>Wire Width, w (mm)</i>	<i>Slot Width, s (mm)</i>
Low Contour	0.6	3.2	0.15
High Contour	1.2	3.2	0.15s

industrial foil-type rotor, such as shown in Figure 3b. The particular foil design used in the CSS rotor had NACA 0015 foils with a 6 degree angle-of-attack. The chord length for this rotor was 4 cm which is comparable to the length of foils used in industrial screens and gives 11 chord lengths per revolution. The gap between the rotor and the wall was set to 2 mm. The second rotor was a non-industrial, solid-core rotor with no elements on its surface and was used to provide a steady circumferential flow within the screen (i.e. without pulsations). The gap between this rotor and the wall was 14.5 mm. The two-dimensional roughness of the lower boundary, i.e. the cylinder surface, was formed by placing the screen wires in a test coupon transverse to the approaching flow. The two test coupons used in these tests are listed in Table 2 considering the slot geometry shown in Figure 2b.

The high-speed video camera was placed in front of the screen coupon with the light source at the rear of the CSS to provide silhouette images of particle motion. Exposure time was set between 10 and 20 μ s. Depth of field was less than 1 mm, which allows the examination of velocity in the flow away from the PlexiglasTM walls of the CSS. Framing rate was set at 20000–54000 frames-per-second (fps). Thus a fibre moving at 10 m/s in the field of view would move approximately 0.25 mm between frames and have a blur of approximately 12 μ m, which is less than a fibre diameter. A 1000 W halogen lamp was positioned at the back of the apparatus. The front cover and a small window on the back side of the CSS were constructed of 25 mm PlexiglasTM plate. The back window was covered by a diffuser for better lighting uniformity. Videos were converted into grey scale images for further analysis. The MATLAB[®] PIVlabTM particle image velocimetry (PIV) utility was used to map the flow field.

Experimental Results

Fibre Trapping Phenomenon

The motion of individual softwood fibres approaching and trapping on the slot edge was recorded and some selected images are shown in Figure 12. The low-contour coupon was used for these tests. Rotor tip velocity was slow relative

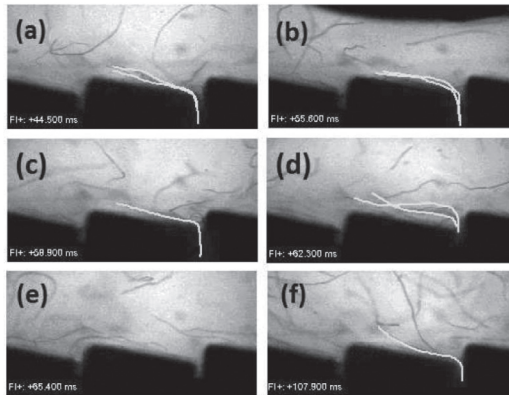


Figure 12. Images of fibres trapping and being cleared by the rotor ($V_t = 5$ m/s, and $V_s = 3$ m/s). The time-wise sequence of shots are recorded relative to $x_r/chord$, which is the distance of the leading edge of the rotor from the upstream edge of the slot divided by the foil chord length: (a) $x_r/chord = -1.0$ (i.e. the rotor foil is approaching the slot and is one chord length away), (b) $x_r/chord = 0.35$, (c) $x_r/chord = 0.6$, (d) $x_r/chord = 1$, (e) $x_r/chord = 1.35$, (f) $x_r/chord = 4.0$ (the rotor foil has passed and the slot is in its distant wake).

to industry norms ($V_t = 5$ m/s versus a more typical 12 to 20 m/s) but this compromise was made to enhance visualization of the fibre motion, with the assumption that the general character of fibre motion would remain unchanged. Slot velocity was 3 m/s.

Many such fibre sequences were recorded and Figure 12 is representative of the observed fibre trajectories. These images challenge the traditional model of the rotor action, which says the maximum suction pressure and release of any fibre accumulation happens with the backflush flow associated with the minimum cylinder-rotor gap (i.e. Figure 12b). What is seen instead is that the release of fibres is delayed until after the rotor passage (Figure 12e) – either because of the delay associated with the inertia of the slot-wise flow and/or because of the reliance on the turbulent wake of the foil for fibre removal.

Steady Flow Analysis

The flow patterns at the slot entry are presented in this section as a function of the contour geometry, rotor speed and slot velocity. This information provides a necessary backdrop to consider a mechanistic model of fibre trapping and release. The smooth rotor was used to provide a steady circumferential flow. A dilute suspension of pulp fines was used as flow tracers.

Fibre trapping is thought to be based on the balance of forces applied to a fibre on the downstream edge of the slot. One force arises from drag on the portion of the fibre length exposed to the mainstream flow parallel to the screen surface. Another force is created by the flow through the slot and drag on the portion of the fibre extending into the slot. The location and character of the vortex adjacent the slot entry is important in determining the position of the stagnation streamline which divides the mainstream and slot flows. Having the stagnation streamline closer to the slot edge may promote trapping since a third force, due to friction of a fibre wrapped around the slot edge, would increase. Having the stagnation streamline closer to the slot edge may also lead to an increased number of shorter fibres becoming candidates for fibre trapping.

The effect of flow conditions and contour height on vortex size are shown in Figures 13 and 14. The figures show a reduction in vortex size and movement of the stagnation point towards the slot entry as slot velocity increases, consistent with Gooding's findings [7]. Vortex size also increases with increased contour height, in agreement with Mokamati *et al.* [19], though the present study suggests the stagnation point is located somewhat closer to the slot entry. The average velocity between the smooth rotor and the screen surface, i.e. V_w , the upstream velocity (m/s), was found to be proportional to rotor speed (i.e. $V_w \sim 40\% V_I$) but independent of the contour height and V_s .

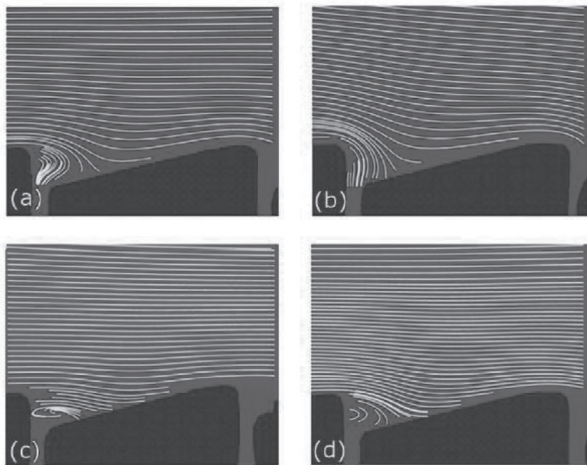


Figure 13. Experimental measurements of flow patterns near a screen slot for steady flow with a low contour: (a) $V_I = 10$ m/s, $V_s = 1$ m/s, (b) $V_I = 10$ m/s, $V_s = 4$ m/s, (c) $V_I = 20$ m/s, $V_s = 1$ m/s, and (d) $V_I = 20$ m/s, $V_s = 4$ m/s.

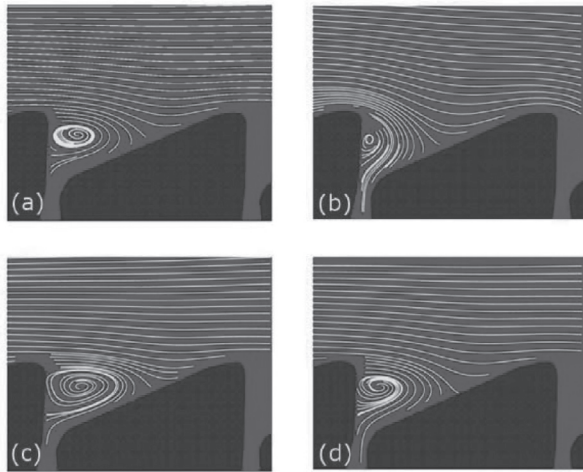


Figure 14. Experimental measurements of flow patterns near a screen slot for steady flow with a high contour: (a) $V_t = 10$ m/s, $V_s = 1$ m/s, (b) $V_t = 10$ m/s, $V_s = 4$ m/s, (c) $V_t = 20$ m/s, $V_s = 1$ m/s, and (d) $V_t = 20$ m/s, $V_s = 4$ m/s.

Higher slot velocities led to increased exit layer thickness, which is significant because this leads to a reduced influence of the “wall effect” [40], an increase in the fibre concentration in the flow going to the slot, and thus an increased rate of fibre trapping and accumulation – which would in turn be a factor in the maximum slot velocity and screen capacity.

The factors examined in this steady-flow part of the study support a model based on the trapping of fibres at a flow bifurcation located near the slot entry, which considers the deposition phase of a capacity model. A time-varying flow analysis is required to consider aspects of the removal phase, which complements the deposition mechanism and is considered below.

Time-Varying Flow Analysis

The rotor foil creates a complex flow field near the wall and is thought to clear fibres from the slot through a combination of: 1) a time-varying wake flow and 2) a pressure pulsation that creates a flow reversal in the slot. Figure 15 shows the rotor-wall geometry used for this study. The foil location is used as a reference for all time-varying data. Figure 16 shows the regions of interests (ROI) where the dynamic u and v velocity components are averaged, as well as the reference plane where spatio-temporal values are assessed. The ROI for the v component is

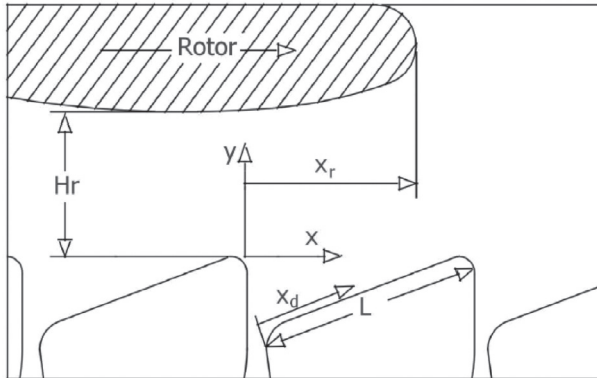


Figure 15. Foil rotor and screen cylinder wall geometry illustrating the variables, H_r , the clearance between the rotor and cylinder (mm), L , the contour length along the top of the wire (mm), x_r , the position of the foil leading edge relative to the upstream edge of the slot (mm) and x_d , the position of the stagnation streamline relative to the downstream edge of the slot (mm).

chosen above the slot since velocity components within the slot could not be evaluated experimentally in this study due to noise and shadow effects. While the ROI for the v component may lie over part of the recirculating zone, it is assumed that the integrated flow across the entry to the contour corresponds to the flow through the slot.

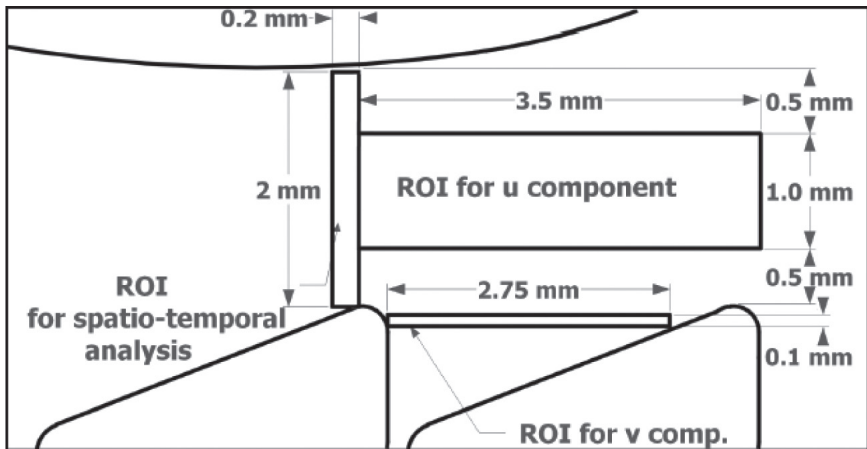


Figure 16. Regions of Interest (ROI) for u and v velocity components.

A trace of the u velocity component is shown in Figure 17 as a function of the position of the rotor (x_r/chord) for a typical screening condition: $V_t = 20$ m/s; $V_s = 1$ m/s. One sees that as the foil approaches the reference slot ($x_r/\text{chord} = -1$) there is no acceleration of the flow; it continues at the average value of $u/V_t \sim 0.58$. When the rotor foil passes over the slot, the u -component of velocity decreases to $u/V_t \sim 0.3$ near the minimum gap between the rotor and cylinder ($x_r/\text{chord} \sim 0.2$). The flow then accelerates under the trailing half of the foil. The highest value of u is seen close to the trailing tip of the foil (i.e. $x_r/\text{chord} = 1$) and the u component of velocity drops back to the average value of u at a distance about two chord lengths behind trailing tip of the rotor (i.e. $x_r/\text{chord} = 3$).

A different perspective on the relationship shown in Figure 17 is given in Figure 18, which shows the changes in the velocity vector field as a function of rotor position. The vector images reinforce what was shown in Figure 17 with the velocity decreasing as the rotor passes ($x_r/\text{chord} = 0.1$) but then rising in the foil wake. The suction pulse generated by a rotor foil is commonly ascribed to a “Venturi flow” or “Bernoulli Effect” whereby the flow accelerates as it passes through the restriction between the foil and screen surface (Hr). The increase in flow velocity is accompanied by a decrease in pressure and this suction pulse generates a backflush flow through the slot that clears away any fibre accumulation.

The notion of an increase in velocity under the foild might appear contrary to the results shown in Figures 17 and 18, which show a decrease in velocity for x_r/chord between 0 and 1. The difference lies in the frame of reference with the flow increase/pressure decrease being based on a frame of reference attached to the foil and application of the steady form of the Bernoulli Equation. The decrease in velocity shown in Figures 17 and 18 follow from a frame of reference attached to the screen surface. A suction pulse naturally still exists, but the analytic approach using a frame of reference on the screen surface would then be based on the unsteady form of the Bernoulli Equation. The porous boundary must also be considered in a rigorous and complete solution.

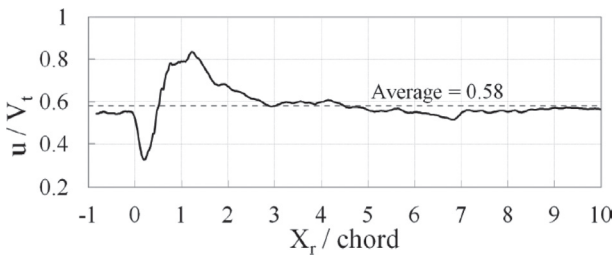


Figure 17. The u component of velocity for the ROI shown in Figure 16 with $V_t = 20$ m/s and $V_s = 1$ m/s.

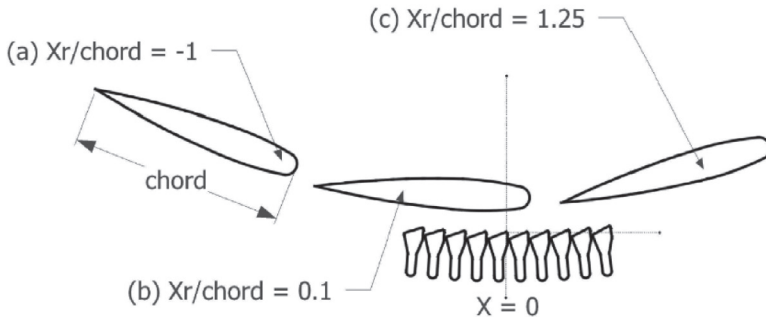
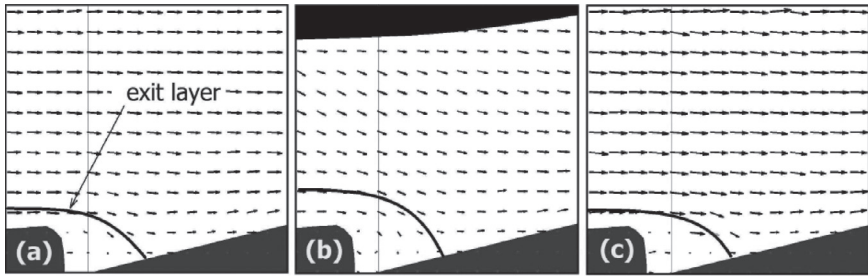


Figure 18. Vector fields for three significant rotor foil positions: (a) the approaching foil, (b) the foil over the reference slot, and (c) the foil wake.

The PIV approach provides a more comprehensive appreciation of the variations in the u component of velocity for not only a range of x_r , but also for a range of distances from the cylinder surface, such as shown in Figure 19. The figure also shows a u -component velocity trace (comparable to Figure 17) and the associated measuring volume. One can see that the average speed of $u/V_t = 0.58$ is represented by a green colour and matches the flow velocity above the slot as the foil approaches ($x_r/\text{chord} < 0$). As one would expect, the flow adjacent the screen cylinder is somewhat slower (shown in blue). When the foil passes, the u component of velocity drops across the full gap between the foil to a value of $\sim 0.3 V_t$, and then rises over the last half of the foil ($0.5 < x_r/\text{chord} < 1.0$) to a value approaching $0.8 V_t$.

The v component of velocity is shown in Figures 20 for a high contour slotted coupon, typical rotor speed of 20 m/s and slot velocities of 1 and 4 m/s. The average value of v is approximately -0.2 m/s, which corresponds to $V_s = 4$ m/s once one accounts for the differences between the widths of the 0.15 mm slot and 2.75 mm v -component ROI (Figure 16). A reversal flow through the slot

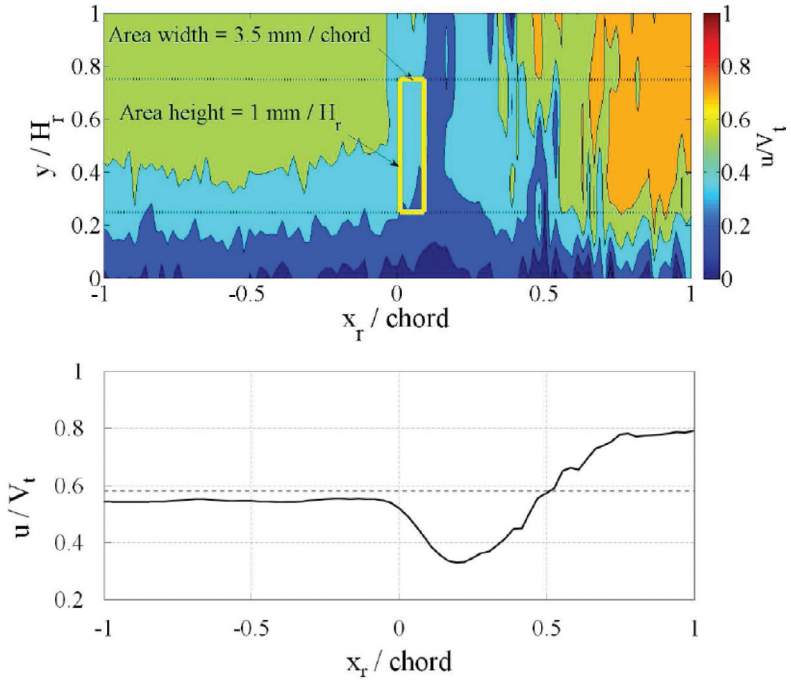


Figure 19. The spatio-temporal description of the u -component in the flow field for a high contour slotted coupon, $V_t = 20 \text{ m/s}$ and $V_s = 1 \text{ m/s}$ (above) along with the measuring volume (in yellow) for averaging. The lower plot is the associated averaged u -component flow velocity.

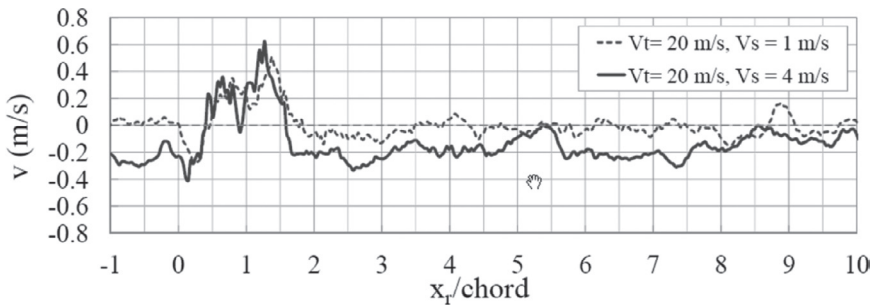


Figure 20. The v -component of velocity for a high contour slotted coupon, $V_t = 20 \text{ m/s}$ and two levels of V_s .

(i.e. positive v component values) is found for $x_t/chord$ between 0.5 and 1.5. While the maximum suction pulse has been assumed to occur with the minimum rotor clearance (i.e. $x_t/chord \sim 0.2$) the reversal flow may be delayed because of fluid inertia. A lower V_s of 1 m/s naturally led to a proportionally lower value of v , but the magnitude, location and duration of the reversal flow was about the same.

A second test configuration considers a low contour and $V_t = 10$ m/s, as shown in Figure 21. In this case, only a small reversal flow is seen where $V_s = 1$ m/s and there is no reversal flow at all when $V_s = 4$ m/s. The implication for industrial screen applications is that plugging may become more problematic when rotor speeds are low and slot velocities are high, as is commonly reported and was seen in Figure 5.

If one assesses the limiting conditions for when a backflush flow occurs, one sees that this threshold is defined by an approximately linear relationship between V_t and V_s , as seen in Figure 22, which is suggestive of the linear $V_t - V_s$ relationship noted in Equation 1. Indeed superimposing the data in Figures 7 and 22 provides a remarkably similar linear relationship, as shown in Figure 23. The occurrence of a backflush flow is, however, insufficient to be entirely predictive of the capacity line. First, Figure 23 shows the threshold of backflushing, i.e. the dashed line between the reversal and non-reversal regimes, to align with the capacity limit of the 2.0% consistency suspension – suggesting that some other factor is acting to limit capacity. Second, a purely flow-based explanation cannot capture the influence of fibre length and concentration, such as seen in Figures 7 and 8. It may be that the turbulent wake flow or flow instabilities also play a role in determining capacity, which will be explored in the following section.

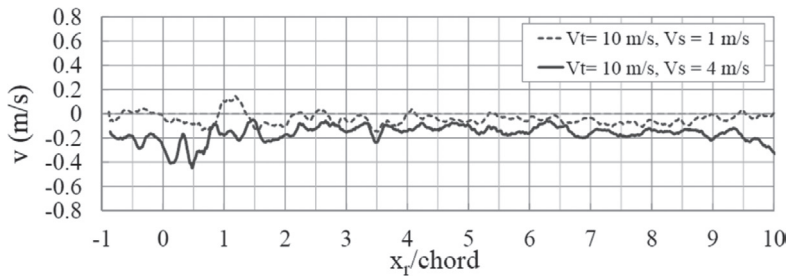


Figure 21. The v -component of velocity for a low contour, $V_t = 10$ m/s and two levels of V_s .

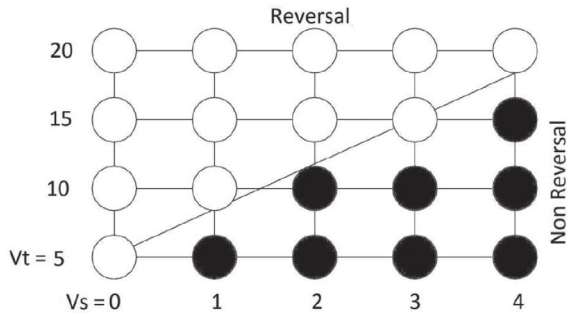


Figure 22. Reversal/Non-reversal flow regimes. The white circles represent test conditions where significant reversal was seen in the flow through the slot.

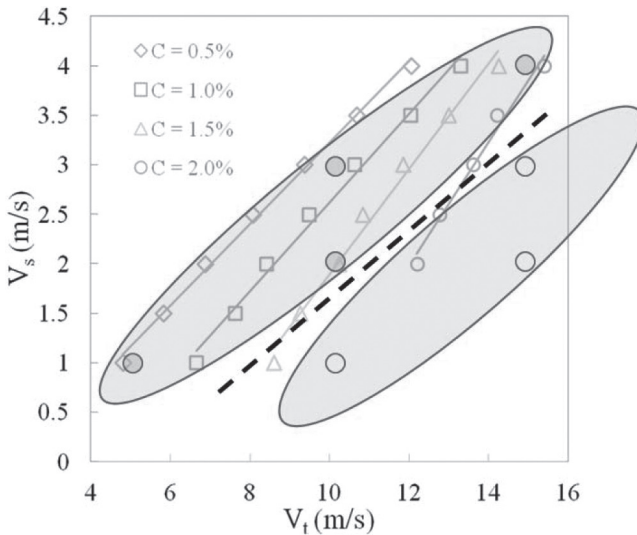


Figure 23. The dashed line signifying the boundary between the non-reversal (shaded) and reversal flow (clear) conditions shown in Figure 22 is superimposed on the capacity curves from Figure 7 to suggest that flow reversal is a significant factor in determining capacity.

Summary of Findings from the Cross-Sectional Laboratory Screen

Tests made with a cross-sectional laboratory screen provided several insights useful to developing a model of capacity. High speed cine images captured the fibre trapping phenomenon, which is proposed as an essential

mechanism in limiting screen capacity. Particle image velocimetry assessed the steady flow patterns within the contour at the entry to the slot as well as the changes in flow related to the passage of the rotor foil. The u -component of flow was seen to decelerate as the flow entered the rotor-cylinder gap and accelerate over the remaining foil length (from a frame of reference fixed to the screen surface). The unsteady flow measurements also showed that a backflush flow did not occur for high slot velocities and low rotor tip speeds.

THEORETICAL MODEL OF SLOT PLUGGING

Trapping of fibres on the downstream edge of a screen slot was seen in Figures 4b and 12 as an essential mechanism leading to screen plugging and thus defining screen capacity. The following analysis extends this to consider a mechanism that complements the action of backflush flows.

The trapping model is based on a force balance for a fibre on the edge of the slot entry. There are three forces on the immobilized fibre: 1) a mainstream drag force induced by the rotor-driven flow, 2) a slot-wise drag force induced by the slot flow, and 3) a friction force acting on the fibre contacting the downstream corner of the slot entry and which resists motion in either the mainstream or slot-wise directions. The fibre remains immobilized as long as the frictional force between the fibre and wire corner exceeds the net drag force, i.e. the absolute value of the difference between the mainstream and slot-wise drag forces.

The approach considered 3 mm fibres initially positioned on the edge of the slot with different proportions of the fibre extending into stream-wise flow. The fibre was divided into 20 segments and drag forces were calculated on each segment. Drag coefficient values at moderate Reynolds Number are provided by Vakil and Green [41] who studied the near-axial flow around two-dimensional cylinders at moderate Reynolds numbers (i.e. $1 < Re < 40$) at various angles between the flow and fibre axis. Flow values for case of the trapped fibre were taken from results of the PIV assessments, such as shown in Figure 13.

To assess the frictional force of a fibre wrapped on a curved surface, Vakil and Green [42] compared the fibre model with the Capstan Equation in either the classical or modified form (see Jung *et al.* [43]). The simple form of the Capstan Equation provides the ratio of tension on the tauter side to the slacker side of a rope wrapping a cylinder as a function of the coefficient of friction and wrap angle. Though the equation is derived for a continuous medium, Vakil and Green applied it to a fibre of discrete length with a finite number of segments and matched the fibre model simulations with the Capstan Equation for low values of friction coefficient and wrap angle. The same approach was adopted here, as shown in Figure 24.

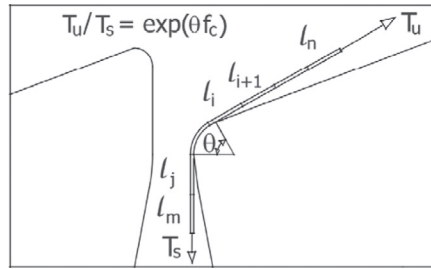


Figure 24. Tensions on a fibre trapped on wire edge with θ equal to the wrap angle of the fibre and f_c which is equal to the coefficient of friction.

A MATLAB[®] code was developed to determine the tension on the fibre portions above and within the slot. Velocity vectors parallel to the fibre were used to calculate drag forces on each segment. The value T_u , the tension on the fibre portion above the slot (kg.m/s^2), was not strongly affected by the slot velocity. It was thus possible to formulate the tension above the slot solely as a function of the velocity component, u , above the screen surface. Figure 25 shows the tension forces on fibre portions above the slot as a function of rotor speed (for the smooth rotor). By normalizing the u component with respect to rotor tip speed, V_t , a single curve was obtained to express the relationship of the u velocity component as a function of foil position for a range of slot velocities.

A curve-fitted equation (Equation 2) was developed to estimate $T_u(i)$ as a function of the rotor position, for the fibre segments above the slot, based on the tension data presented in Figure 25:

$$T_u(i) = [0.71 (u/V_t)V_t + 0.3l(i)^2 + 0.92 (u/V_t)V_t - 0.02l(i) - 0.75] \cdot 10^{-6} \quad (2)$$

The total drag force on the mainstream fibre portion (above the slot) follows as:

$$T_u = \sum_{i=1}^n T_u(i) \quad (3)$$

The drag force on the fibre within the slot was calculated using the local slot velocity, i.e. the total slot flow divided by the width of the slot at the particular location of each fibre segment. The nominal slot velocity, V_s , is the value in the slot “throat” (i.e. the minimum slot width). The throat length is typically much shorter than the fibre length and the slot throat is typically followed by an expansion section. This correction assumes an orderly expansion of flow through the slot and does not consider jet flows, recirculating zones in either the expansion

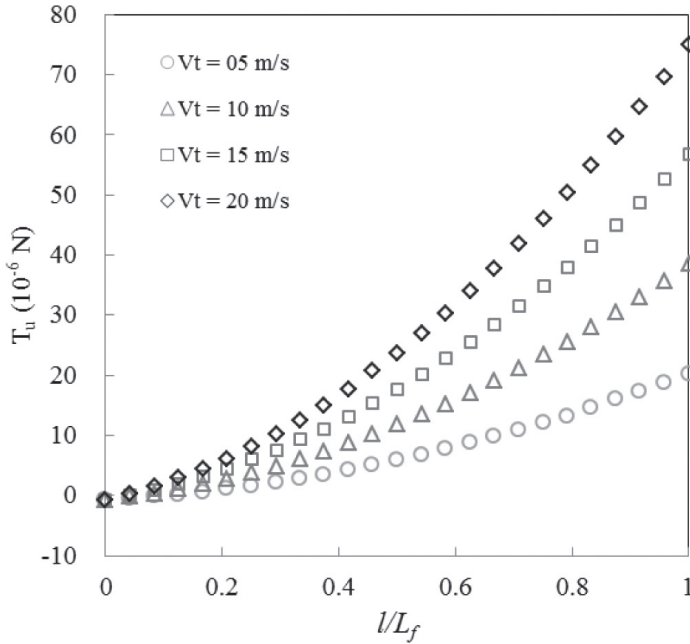


Figure 25. Tension forces on the fibre portion above the slot as a function of the (smooth) rotor speed (V_t).

section or the slot itself, or other complexities which have been reported in the literature [19]. Another significant simplifying assumption is that the accumulation of the fibres within the slot is assumed to not affect the local slot velocities. Three-dimensional effects have also been excluded from the analysis.

Using the local slot velocity and the C_D values from Vakil and Green [41], the total drag force can be integrated over the slot-wise fibre length:

$$T_s = \sum_{j=1}^n T_s(j) \tag{4}$$

where

$$T_s(j) = \frac{1}{2} \rho v(j)^2 C_D(i) D l(j) \tag{5}$$

By examining the force difference, $|T_u - T_s|$, as a function of rotor position and comparing this to the friction force exerted on the fibre at the wire corner, one can

determine whether the fibre will be immobilized (trapped) or shed in either the mainstream or slot-wise direction. The possibility of the fibre repositioning itself on the slot edge to achieve a stable position was excluded from this analysis. The component forces, force difference and friction force are all shown in Figure 26 for a 3 mm fibre initially positioned on a low contour wire edge and with $V_i = 5$ m/s and $V_s = 2$ m/s. In this particular example, fibres that were initially deposited with the position of $0.50 < l/L < 0.67$ would remain trapped, while fibres deposited with a value of l/L outside this range would be shed. For trapped fibres to accumulate within the slot requires that V_i does not change to the extent that the range of values for l/L that prescribe the trapping condition shift so that the originally trapped fibres are released.

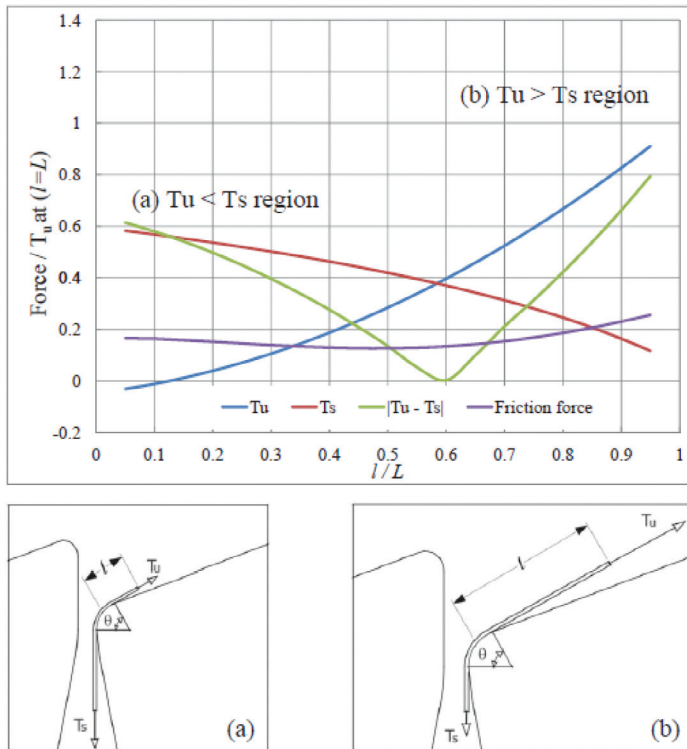


Figure 26. Fibre force balance as a function of trapped fibre position.

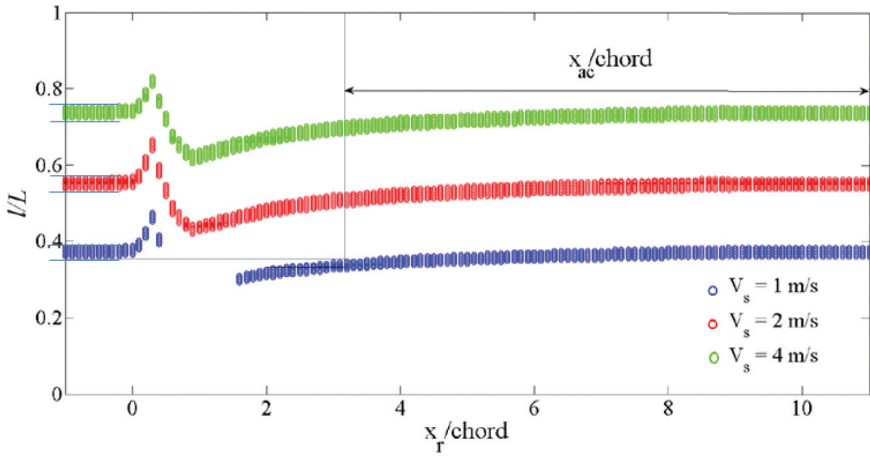


Figure 27. Accumulation of 3 mm fibres on a low contour wire during a foil cycle with $V_t = 10$ m/s.

The accumulation of 3 mm fibres within a slot is shown in Figure 27 for three slot velocities. For $V_s = 1$ m/s, there is a narrow band of $//L$ possibilities, i.e. between 0.38 and 0.40 ($\sim 2\%$ of the possible range) that will become trapped. As the rotor foil passes, the band moves significantly and there is a reverse flow that is assumed to release all trapped fibres. At $x_r / chord \sim 3$, the mainstream flow has stabilized so that fibres can accumulate until the return of the foil passage, i.e. the $//L$ band does not shift more than the width of the band. This period of accumulation is designated as $x_{ac} / chord$. A similar sequence of events is seen for $V_s = 2$ m/s and $V_s = 4$ m/s except that there is no reverse flow in the two other cases.

The width of the $//L$ band and the initial point of the $x_{ac} / chord$ interval are approximately the same for all three cases. This suggests that the initiation of plugging will increase linearly with lower rotor speeds given that the time per revolution (or time per chord length) will increase linearly, allowing for increased deposition of fibres. Plugging would also be expected to increase linearly with higher slot velocities since the delivery of fibres to the slot edge will increase proportionally.

The model of fibre trapping can be extended to consider zones of accumulation and release. Screen capacity can, in turn, be modelled as the case where: 1) there is no backflush flow and 2) fibres accumulate and fill the slot before the release phase occurs. As discussed in reference to Figure 23, the backflushing action which has traditionally been considered essential to the release phase may be supplemented by the action of a turbulent wake flow or, as discussed in reference to

Figure 27, flow instabilities which move the instantaneous value of l/L so that previously trapped fibres are shed.

What is most critical to this trapping-capacity model is the accumulation of fibres. It follows from the above force balance that given the critical l/L band is relatively constant in width and that the $x_{ac}/chord$ interval is relatively constant in length, one can develop a fibre Accumulation Number, N_{ac} , as described in Equation 6. In particular, and as a first-order approximation, the equation assumes that the delivery of fibres to the trapping location is proportional to the slot velocity, V_s , and upstream consistency, C_U . The percentage of delivered fibres that impact the downstream slot edge with a value of l/L within the band that produces trapping was found above to be relatively constant and is embraced within the constant, k_1 . The time for the build-up of fibres is proportional to the length accumulation zone, $x_{ac}/chord$ as seen in Figure 27 (with the simple conversion of chord length to distance also being embedded within k_1) and inversely proportional to upstream velocity, which is related by a constant to rotor tip speed, V_t .

$$N_{ac} = [C_U V_s] \left[\frac{x_{ac}}{chord} \frac{1}{V_t} \right] k_1 \quad (6)$$

To extend Equation 6 to a representation of the linear relationship shown, for example, in Figure 7 requires the consideration of several key factors:

- Slot width, which complements the accumulation number with a threshold that indicates when plugging occurs. This will also introduce the offset seen previously in V_s-V_t relationships.
- Differentiating between the overall fibre consistency and the longer fibre fraction which are candidates for trapping.
- Distinguishing between the upstream and screen feed consistencies.
- Introducing a factor to account for the shedding of trapped fibres because of rotor foil wake effects.

The inclusion of these factors is anticipated to yield a linear $V_t - V_s$ relationship which will relate the essential elements of the fibre trapping force balance to industrial screen capacity and is the next step in this line of research.

SUMMARY AND CONCLUSIONS

The objective of this study was to develop a fundamental understanding of factors that determine the capacity of modern pulp screens. The trapping of a fibre on a solid edge with friction and in the presence of an adjacent flow bifurcation was

identified as the essential mechanism underlying screen capacity, and that became the basis of the study. In essence, fibres accumulate on the downstream edge of the slot, with an adjacent cross-flow, when the difference in drag force applied on fibre portions above and within the slot is smaller than the fibre-wall friction force. Fibres build up with time until a disturbance in the flow field is introduced. The disturbance may be major, such as the backflush flow generated by the rotor, but it may also be minor, such as flow structures in the wake of a rotor foil or variations in the crossflow which eliminate the possibility of trapping. Trapping thus defines a time-dependent phenomenon of accumulation and release which can, in one extreme, lead to slot plugging and screen failure.

The fibre trapping phenomenon had been reported in the literature in the context of other pulp and paper applications, but was observed in the present study in a laboratory device which simulated the flows near a slot in a pulp screen. An analytic model was created to consider the likelihood of fibre trapping as well as the stability of the flow bifurcation in a flow environment representative of the flow near a pulp screen slot. The rate of growth of trapped fibres relative to the width of the slotted aperture in a pulp screen was seen as essential to the screen plugging phenomenon and the basis of a linear relationship of two key industrial variables driving the two bifurcating flows: the slot velocity and the rotor tip speed.

A laboratory study of the flows near a screen slot was conducted in support of this model based on high-speed photography and particle velocimetry. The findings of this experimental study yielded the flow field required to consider when trapping would occur. Dynamic measurements of the flow associated with the passage of the rotor foil, showed that there was a consistent, albeit narrow, range of conditions that would lead to trapping of fibres. These conditions provided the opportunity for significant growth of the fibre accumulations in the time frame defined by the passage of the rotor foils. The more traditional model of screen capacity, based on backflushing of the slot, was found to be limited and unable to fully account for screen capacity given that it is not sensitive to such important factors as fibre length distribution and that, in certain cases, backflushing was not observed under flow conditions where screens could operate reliably.

Pilot plant studies provided guidance in identifying the factors relevant to screen capacity. A highly linear relationship between slot velocity and rotor tip speed was repeatedly seen, and it is this curve that defines the screen capacity limitations. The linear relationship persisted even as changes in fibre length distribution and consistency were seen to shift the particular location of the line. The importance of factors such as screen reject ratio and, cylinder contour height, were documented, which provides context for the more fundamental analysis.

This study has thus reduced a complex and important industrial problem to a more fundamental problem, which is believed to be of essential importance in defining screen capacity. The studies of fibre trapping may well be relevant to

other fields. The practical insight into capacity promises to be of immediate use in mill operations by understanding the operational factors that can be used to increase capacity, or to reduce slot size or rotor speed for quality and energy savings, without compromising capacity. A framework is also provided for the development of improved pulp screening equipment and further study.

Thus, while a comprehensive understanding of pulp screen capacity remains elusive, the present research has provided insights which move away from the simplistic “backflush” models used in the past and supports a more sophisticated model that also considers: 1) the dynamics of fibre deposition and removal rates at the slot entry, 2) the importance of small-scale perturbations created by turbulent flow for fibre removal, and 3) the mechanisms of fibre trapping on the downstream edge of the slot. This more comprehensive model provides direction for future development.

In particular, future work should broaden the theoretical analysis to consider a range of fiber lengths and to provide predictions of when the slot would be filled prior to the backflushing/disruptive pulse. Laboratory (CSS) and pilot plant studies would then consider a range tests with rotor foil designs chosen to decouple the effects of pulsation, wake turbulence and trapping disruption in order to test this capacity model and explore possible industrial screen rotor designs.

REFERENCES

1. R.W. Gooding and R.J. Kerekes. The motion of fibres near a screen slot. *J. Pulp Paper Sci.* **15**(2):59–62, 1989.
2. A. Kumar. The passage of fibres through screen apertures. Ph.D. thesis, The University of British Columbia, Canada, 1991.
3. J.A. Olson and G.W. Wherrett. A model of fibre fractionation by slotted screen apertures. *J. Pulp Paper Sci.* **24**(12):398–402, 1998.
4. C.J. Yu and R.J. DeFoe. Fundamental study of screening hydraulics. Part 1: Flow patterns at the feed-side surface of screen baskets; mechanism of fiber-mat formation and remixing. *Tappi J.* **77**(8):219–226, 1994a.
5. C.J. Yu and R.J. DeFoe. Fundamental study of screening hydraulics. Part 2: Fiber orientation in the feed side of a screen basket. *Tappi J.* **77**(9):119–124, 1994b.
6. R.W. Gooding and D.F. Craig. The effect of slot spacing on pulp screen capacity. *Tappi J.* **75**(2):71–75, 1992.
7. R.W. Gooding. Flow resistance of screen plate apertures. Ph. D. thesis, The University of British Columbia, Canada, 1996.
8. J.A. Olson. The effect of fibre length on passage through a single screen aperture. Ph. D. thesis, The University of British Columbia, Canada, 1996.
9. A. Yong, S. Mokamati, D. Ouellet, R.W. Gooding and J.A. Olson. Experimental measurement of fibre motion at the feed surface of a pulp screen. *Appita J.* **61**(6): 485–489, 2008.

10. J. Jimenez. Turbulent flows over rough walls. *Ann. Rev. Fluid Mech.* **36**:173–196, 2004.
11. V.C. Patel. Flow at high Reynolds Number and over rough surfaces-Achilles heel of CFD. *ASME J. Fluid Eng.* **120**:434–444, 1998.
12. P. Bradshaw and F.Y.H. Wong. The reattachment and relaxation of a turbulent shear layer. *J. Fluid Mech.* **52**:113–135, 1972.
13. G. Gregoire, M. Faver-Marinet and F. Julien Saint Amand. Modeling of turbulent fluid flow over a rough wall with or without suction. *Trans. ASME* **125**:636–642, 2003.
14. O. Heise. Screening foreign material and stickies. *Tappi J.* **75**(2):78–81, 1992.
15. J. Niinimäki, O. Dahl, H. Kuopanportti and A. Ammala. Comparison of pressure screen baskets with different slot widths and profile heights – selection of the right surface for a groundwood application. *Paperi ja Puu* **80**(8):601–605, 1998a.
16. L. Halonen, R. Ljokkoi and K. Peltonen. Improved screening concepts. In proc. *Tappi Pulping Conf.* pp 61–66, Seattle, Washington, 1989.
17. F. Frejborg. Improved operation of TMP plant through optimization of screening. *Pulp Paper Canada* **89**(1):107–112, 1989.
18. T. Bliss. Screening in the stock preparation system. In proc. *Tappi Stock Preparation Short Course*, pp 59–75, Atlanta, Georgia, 1990.
19. S. Mokamati, J.A. Olson and R.W. Gooding. Numerical study of separated cross-flow near a two-dimensional rough wall with narrow apertures and suction. *Can. J. Chem. Eng.* **88**(1):33–47, 2010.
20. C.J. Yu, R.J. DeFoe and B.R. Crossley. Fundamental study of screening hydraulics. Part 3: Model for calculating effective open area. *Tappi J.* **77**(9):125–131, 1994c.
21. R.J. Kerekes. Pulp floc behavior in entry flow to constrictions. *Tappi J.* **66**(1):88–91, 1983.
22. S. Blaser. Flocs in shear and strain flows. *J. Colloid and Interface Sci.* **225**(2): 273–284, 2000.
23. T. Paul, G. Duffy and D. Chen. Viscosity control as a new way to improve pressure screen performance. *Tappi J.* **83**(9):61–100, 2000.
24. J.A. Olson and R.J. Kerekes. Motion of fibres in turbulent flow. *J. Fluid Mech.* **377**:47–64, 1998.
25. R. Karvinen and L. Halonen. The effect of various factors on pressure pulsation of a screen. *Paperi ja Puu* **66**(7):80–83, 1984.
26. V. Pinon, R.W. Gooding and J.A. Olson. Measurements of pressure pulses from a solid core screen rotor. *Tappi J.* **2**(10):9–12, 2003.
27. S. Levis. Screening of secondary fibers. *Progress in Paper Recycling* **1**(1):31–45, 1991.
28. J. Niinimäki, A. Ammala, H. Kuopanportti and S. Nissila. The settings of hydrofoils in a pressure screen. In proc. *Int. Symposium on Filtration*, pp 71–78, Las Palmas, Canary Islands, 1998.
29. M. Feng, J. Gonzalez, J.A. Olson, C. Ollivier-Gooch and R.W. Gooding. Numerical simulation and experimental measurement of pressure pulses produced by a pulp screen foil rotor. *J. Fluids Eng.* **127**(2):347–357, 2005.
30. S. Delfel, J. A. Olson, C. Ollivier-Gooch and R.W. Gooding. Effect of pulse frequency and cylinder diameter on pressure screen rotor performance. In proc. *65th Appita Ann. Conf.*, pp 89–96, Rotorua, New Zealand, 2011.

31. C. McCarthy. Various factors affect pressure screen operation and capacity. *Pulp and Paper* **62**(9):233–237, 1988.
32. D. M. Martinez, R. W. Gooding and N. Roberts. A force balance model of pulp screen capacity. *Tappi J.* **82**(4):181–187, 1999.
33. H. Jokinen, A. Ammala, J. A. Virtanen, K. Lindroos and J. Niinimäki. Pressure screen capacity – current findings on the role of wire width and height. *Tappi J.* **6**(1):3–10, 2007.
34. M. Hamelin, S. Delfel, J. Olson, C. F. Ollivier-Gooch and R. Gooding. High performance multi-element foil (MEF) pulp screen rotor – Pilot plant and mill trials. *J. Pulp Paper Sci.* **36**(3–4) 2011.
35. J. Niinimäki. Phenomena affecting the efficiency of a pressure screen. In proc. *Tappi Pulping Conf.* pp 957–966, 1999.
36. A. Konola, I. Poikolainen, K. Kovasin, J. Karppinen and R. Gooding. Reduced power consumption in softwood kraft screening at Botnia Aankoski. *Paperi ja puu* **91**(3):27–32, 2009.
37. F. Julien Saint Amand and B. Perrin. Fundamentals of screening: Experimental approach and modelling. In proc. *Tappi Pulping Conf.* pp 1019–1031, Montreal, Canada, 1998.
38. R.W. Gooding and R.J. Kerekes, Consistency changes caused by pulp screening. *Tappi J.* **75**(10):109–118, 1992.
39. J. Gonzalez. Characterization of design parameters for a free foil rotor in a pressure screen. M.A.Sc. thesis, The University of British Columbia, Canada, 2002.
40. R. W. Gooding. The passage of fibres through slots in pulp screening. M.A.Sc. thesis, The University of British Columbia, Canada, 1986.
41. A. Vakil and S. Green. Flexible fiber motion in the flow field of a cylinder. *Int. J. of Multiphase Flow* **37**(2):173–186, 2011.
42. A. Vakil and S. Green. Drag and lift coefficients of inclined finite circular cylinders at moderate Reynolds numbers. *Computers and Fluids* **38**(9):1771–1781, 2009.
43. J. H. Jung, N. Pan and T. J. Kang. Capstan equation including bending rigidity and non-linear frictional behavior. *Mechanism and Machine Theory* **43**(6):661–675, 2008.

Transcription of Discussion

SOME FUNDAMENTAL ASPECTS OF PULP SCREEN CAPACITY

H.J. Salem,^{1,2} *R.W. Gooding*,^{1,2,4} *D.M. Martinez*^{2,3} and
J.A. Olson^{1,3}

¹ Department of Mechanical Engineering
The University of British Columbia
6250 Applied Science Lane
Vancouver, British Columbia, Canada V6T 1Z4

² The Pulp and Paper Centre
The University of British Columbia
2385 East Mall
Vancouver, British Columbia, Canada V6T 1Z4

³ Department of Chemical and Biological Engineering
The University of British Columbia
2360 East Mall
Vancouver, British Columbia, Canada V6T 1Z3

⁴ Aikawa Fiber Technologies
5890 Monkland Avenue, Suite 400
Montreal, Quebec, Canada H4A 1G2

Jean-Claude Roux Grenoble Institute of Technology-Pagora

This is interesting work on the importance of the engineering parameters and you showed wonderful pictures of fibres going through slots. If I correctly understand your point of view, you want to reduce the tangential velocity to improve energy consumption, and you also want to increase the velocity through the slots in order to increase the capacity of the pulp screen. You showed us some stagnation streamlines around the slot. Have you investigated whether you can change, for example, the radius of curvature of the micro-geometry at the slot entry in order to move these stagnation streamlines, and what do you think about this idea?

Discussion

Robert Gooding

That is a very perceptive comment. We did look at, perhaps, six different angles of the wire contour which would affect the streamlines. Thus we did not look at anything novel in terms of changing the shape of the contour, but we looked at higher contours, lower contours and essentially different angles. The issue of the contour is tough to pull apart; you have the effect on the fibre trapping position, the stagnation streamline and the passage of fibres through the length of the screen – remembering that the triggering point of screen plugging is at the reject end of the screen. We thus see that the micro-geometry is tangled into a lot of performance parameters.

Jean-Claude Roux

Okay, so you mean that the contour micro-geometry does not change the trapping mechanism? Trapping occurs even if we change the position of the stagnation streamlines?

Robert Gooding

Within the realm of industrial wire shapes, we always saw the trapping; we always saw the stagnation streamline. Trapping became more pronounced with the lower contour as you would expect. Ultimately, with no contour at all, fibres trap very, very quickly and the screen fails very quickly. We did the set of tests with the different contours, as I mentioned previously, and we found what you would expect. That said, I think your point about the potential for a novel shape is an interesting one.

Michael Schneeberger Graz University of Technology

I have two questions. First, in practice we want good screening results: we want low energy, low maintenance costs and good runnability. Where do you see the biggest potential concerning the application of your research in industrial screens? Where do you see a potential to make further improvements in industrial screens? The second question is that you showed very nice video where we could see the fibres in the screen, is it possible to get this video for our students?

Robert Gooding

We are studying the best way to distribute these videos. We have branded a couple with the logos of AFT, UBC to acknowledge the sponsoring organisations, but what we would ultimately want is to have people benefit from the videos.

On the first question, on what is the greatest value of screening research: you really have to tune that to the particular mill and what should be developed is a pie chart of the total cost of contaminants. For some people cost is dominated by the cost of having to buy a cleaner furnish, if you have a recycled paper mill, or having to accept more fibre loss, or, for some people, requirements are driven by energy costs. The nice thing about capacity is that it is the currency that you have to buy each of those things. I mentioned earlier, if you have excess capacity or the ability to operate at a higher capacity, you can slow down the rotor to save power, or you can increase the debris removal efficiency by using a smaller slot. So I think it is a pretty dynamic question of what an individual mill would want, and the nice thing is to have the tools to say how that benefit could be delivered to that mill. Concerning the question of further developments: the greatest potential for research is in the optimal combination of rotor shapes and wire shapes. There is some potential for novel materials, but the greatest opportunities exist more in dealing with geometric issues right now.

Juha Salmela VTT

Could you comment on one thing? You showed in the particle tracking section that there is a region of interest for the V- direction component which is at the top of the slot. On the other hand, it is very close to both the stagnation point that you showed and the eddy at the slot entry, which are both quite unstable, I would think. Do you believe that region of interest might have some effect on a back-flush effect not being observed?

Robert Gooding

You are very perceptive. In one case, I am saying that we assume that everything that passes into the contour entry is going to go through the slot. At the same time I am saying there is a stagnation streamline which cuts across the contour entry and not all particles are moving to the slot. That is indeed a limitation of this approach. It was our first use of that technique, and that would certainly be an opportunity for more refinement and a more accurate measurement of the slot flow in the future. That aside, I do not believe the instability of the flow would lead to an absence of back-flush flow.

Asaf Oko SP Technical Research Institute of Sweden

You showed in your model that the fibres are trapped on the contour wall. In that model, did you also include the friction force between the fibre and the wall?

Discussion

Robert Gooding

Yes. The friction force is based on the tension applied to the fibre by drag from the upstream and slot flows, and the vector sum of those forces applied to the corner of the slot.

Asaf Oke

Can you conclude how important friction is in that mechanism? Would some change in the surface chemistry of that wall, reducing friction, be significant?

Robert Gooding

I think that is an interesting possibility – by perhaps reducing the friction coefficient of the metal surface, or the character of the fibre, or by changing the geometry of the slot edge. I think that is an interesting possible direction of the research. This research is valuable not just for its immediate findings, but to help us identify the most promising opportunities for future work.

Daniel Söderberg KTH and Innventia (from the chair)

There is a suggestion of a combined capacity parameter when looking at the figures that consider capacity as a function of fibre concentration and fibre length. This seems to relate to the crowding number concept. I did the calculation, and the movement you have of the line from 1% to 0.5% concentration is the same as you would get if you decreased fibre length by having pure hardwood. The crowding number may be useful here since it depends both on concentration and on the number of fibres present.

Robert Gooding

As you and I have discussed previously, fibre concentration alone does not drive flocculation, and likewise it does not alone drive the capacity in a screen. Concentration is, however easy to measure, and so it is commonly used. A very tempting avenue for future research is to determine the key parameter driving capacity, that would let the curves in the figures collapse onto a single line. That might depend on concentration of long fibres, for example.